Journal of the Korean Nuclear Society
Volume 32, Number 4, pp.361~371, August 2000

Calculation of Proton-Induced Reactions on Tellurium Isotopes Below 60 MeV for Medical Radioisotope Production

Doohwan Kim and Jonghwa Chang
Korea Atomic Energy Research Institute
150 Dukjin-dong, Yusong-gu, Taejon 305-353, Korea
dookim@lui.kaeri.re.kr

Yinlu Han
China Institute of Atomic Energy,
275(41), 102413, Beijing, P.R. China

(Received February 9, 2000)

Abstract

The $^{123}Te(p,n)^{123}I$, $^{124}Te(p,n)^{124}I$ and $^{124}Te(p,2n)^{123}I$ reactions, among the many reaction channels opened, are the major reactions under consideration from a diagnostic purpose because reaction residuals as the gamma emitters are used for most radiophamaceutical applications involving radioiodine. Based on the available experimental data, the absorption cross sections and elastic scattering angular distributions of the proton-induced nuclear reaction on Te isotopes below 60 MeV are calculated using the optical model code APMNK. The transmission coefficients of neutron, proton, deuteron, trition and alpha particles are calculated by CUNF code and are fed into the GNASH code. By adjusting level density parameters and the pair correction values of some reaction channels, as well as the composite nucleus state density constants of the pre-equilibrium model, the production cross sections and energy-angle correlated spectra of the secondary light particles, as well as production cross sections and energy distributions of heavy recoils and gamma rays are calculated by the statistical plus pre-equilibrium model code GNASH. The calculated results are analysed and compared with the experimental data taken from the EXFOR. The optimized global optical model parameters give overall agreement with the experimental data over both the entire energy range and all tellurium isotopes.

Key Words : nuclear data, medical radioisotope production, proton reaction, 60 MeV, code evaluation

1. Introduction

Medical radioisotopes are used for diagnostic and therapeutic purposes, as well as for metabolism and physiological function research in modern medicine. The excitation functions in

charged particle nuclear reactions governing medical radioisotope production are measured with the aid of either a residual nucleus activity method or outgoing particle measurement method. In the nuclear reaction for medical radioisotope production, the unwanted isotopes are parasitically produced by the accompanying reaction channels. The cross sections for these parasitic-productions should be evaluated for the exact estimation of the cross sections for the wanted productions.

The radioisotope ^{123}I, having a short lifetime ($T_{1/2}$ = 13.3 hours) as compared to the lifetime of the more commonly used ^{131}I ($T_{1/2}$ = 8 days), is one of the best radionuclides in use for *in-vivo* measurements using single photon emission computed tomography (SPECT). It is known that when ^{123}I is used with high material purity, one can reduce the required radiation exposure level applying to the patient and obtain high quality scintiphotos. ^{124}I ($T_{1/2}$ = 4.18 days), which is the only longer-lived β^+ emitting radioisotope of iodine, is widely utilized for labelling biomolecules, especially in tumour research. A therapeutic purpose is achieved by its high radiation dose (comparable to that from ^{131}I), and a diagnostic application is also favored because of the uptake kinetics of iodo-radiopharmaceuticals, via positron emission tomography (PET). From these aspects, several nuclear reactions associated with ^{123}I and ^{124}I productions have been studied. However, the ^{123}I production by direct nuclear reactions always results in the production of radionuclidic impurities of ^{124}I, ^{125}I, ^{130}I, etc. at various impurity levels. An evaluation for unwanted isotope production is not negligible for the evaluation for the major production reaction considered.

In the past work [1], the proton-induced reactions on Ti, Fe, Cu and Mo were calculated for the cross sections at the energy range below 60 MeV for TLA Application. In the present work, based on available experimental data, the proton-induced nuclear reaction cross sections of $^{122,123,124,125,126,128,130,nat}Te$ below 60 MeV are evaluated by using the optical model code APMNK [2] and the statistical plus pre-equilibrium model code GNASH [3]. The absorption cross sections and elastic scattering distributions are calculated by the APMNK code. The transmission coefficients of neutron, proton, deuteron, trition and alpha particles are calculated by the CUNF code [4] and are fed into the GNASH code. The decay processes including n, p, d, t and α particles are theoretically calculated by the GNASH code. The GNASH code is used to calculate all particle emission cross sections, production cross sections and the energy-angle correlated spectra of secondary light particles as well as the production cross sections and energy distributions of heavy recoils and gamma rays. Among the many reaction channels, the $^{123}Te(p,n)^{123}I$, $^{124}Te(p,n)^{124}I$ and $^{124}Te(p,2n)^{123}I$ reactions are the major reactions under consideration for diagnostic purposes because reaction residuals as gamma emitters are used for most radiophamaceutical applications involving radioiodine. The results are compared with the experimental data taken from the EXFOR.

2. Calculation Model

The optical model is one of the most important theories in nuclear data calculations. The evaporation model describing the compound nucleus process and the exciton model describing the pre-equilibrium emission process, require the transmission coefficient T_{lj} and the compound nucleus formation cross section, which should also be calculated by the optical model. The calculated results using the optical model strongly depend on the global potential parameters in the optical potential model. Thus, adjustment of the optical

model parameters is the crucial step in nuclear data calculations.

In the study, the optical potential is based on four forms; the Woods-Saxon form for the real part and imaginary volume absorption part, the derivative Woods-Saxon form for the imaginary volume absorption part, the Thomas form for the spin-orbit part and the Coulomb interaction part. The charged particle optical potential $V(r)$ is as follows:

$$V(r) = - Vf_r(r) - iW_V f_V(r) + 4ia_S W_S \frac{df_S(r)}{dr} + \frac{\lambda_\pi^2}{r} V_{so} \frac{df_{so}(r)}{dr} (\vec{\sigma} \cdot \vec{l}) + V_C(r), \quad (1)$$

where

$$V = V_0 + V_1 E + V_2 E^2 + V_3 \frac{(N-Z)}{A} + V_4 \frac{Z}{A^{1/3}}, \quad (2)$$

$$W_S = W_0 + W_1 E + W_2 \frac{(N-Z)}{A}, (W_S \leq 0), \quad (3)$$

$$W_V = U_0 + U_1 E + U_2 E^2, (W_V \leq 0), \quad (4)$$

$$V_C(r) = \begin{cases} \frac{zZe^2}{2R_C}(3 - \frac{r^2}{R_C^2}) & r < R_C \\ \frac{zZe^2}{r} & r \geq R_C \end{cases}, \quad (5)$$

$$R_i = r_i A^{1/3} \quad i = r, S, V, SO, \quad (6)$$

$$a_i = a_{i0} + a_{i1} \frac{N-Z}{A} \quad i = S, V. \quad (7)$$

E is the incident proton energy in the laboratory system. λ_π is the Compton wavelength of a pion, $\lambda_\pi^2 \approx 2$ fm^2, and the form factors are of the standard Woods-Saxon form: $f_i(r) = \frac{1}{1+exp[(r-R_i)/a_i]}$. The quantity $\vec{\sigma} \cdot \vec{T}$ is the scalar product of the intrinsic and orbital angular momentum operators. R_i and a_i are the radii and the diffusion widths respectively. The 17 parameters, V_0, V_1, V_2, V_3, V_4, W_0, W_1, W_2, U_0, U_1, U_2, r_r, r_s, r_v, a_r, a_s, and a_v should be adjusted.

The APMNK code has a function of automatic search for the optimized parameter values in the charged particle optical potentials utilizing experimental data. The fastest falling method is applied in fitting for the angle-dependent elastic cross section data and the energy-dependent absorption cross section data for medium-heavy nuclei upto an energy of 300 MeV. The spherical optical potential is used to calculate the total cross section, shape elastic scattering cross section and its angular distribution, absorption cross section and transmission coefficients. The compound nucleus elastic scattering distributions are calculated by using the width fluctuation corrected Hauser-Feshbach theory.

The optical potential parameters are automatically optimized with a minimized χ^2, which represents the deviation of the calculated non-elastic cross-section and elastic scattering distribution from the corresponding experimental values. χ^2 is defined as follows:

$$\chi^2 = \frac{W_{ne}\chi^2_{\sigma_{ne}} + W_{el}\chi^2_{\sigma_{el}(\theta)}}{W_{ne} + W_{el}}, \quad (8)$$

where

$$\chi^2_{\sigma_{ne}} = \frac{1}{N_{ne}} \sum_{j=1}^{N_{ne}} [\frac{\sigma^T_{ne}(j) - \sigma^E_{ne}(j)}{\Delta\sigma^E_{ne}(j)}]^2, \quad (9)$$

$$\chi^2_{\sigma_{el}(\theta)} = \frac{1}{N_{el}} \sum_{j=1}^{N_{el}} \frac{1}{n_j} \sum_{i=1}^{n_j} [\frac{\sigma^T_{el}(\theta_{ji}) - \sigma^E_{el}(\theta_{ji})}{\Delta\sigma^E_{el}(\theta_{ji})}]^2. \quad (10)$$

The superscripts T and E represent the theoretical and experimental values, respectively. The values of N_{ne} and N_{el} are the numbers of energy points of the experimental data for a non-elastic cross-section and elastic scattering distribution, corresponding to σ_{ne} and $\sigma_{el}(\theta)$, respectively. n_j is the number of angles of the experimental

differential cross sections corresponding to the j-th energy point, and θ_{ji} is the angle value of the i-th angle for the j-th energy point. W_{ne} and W_{el} are weight factors. There are no total cross sections for the incident charged particles, the reaction (non-elastic) cross sections and the elastic scattering distributions are only taken into account.

A calculation for equilibrium emissions was performed by the Hauser-Feshbach theory with full angular momentum and parity conservation. The pre-equilibrium theory was used for describing the processes of pre-equilibrium emission and damping to equilibrium. Compound reaction calculations with pre-equilibrium corrections were performed using the GNASH code based on the excitation model of Kalbach [5], discrete level data from nuclear data sheets, continuum level densities using the formulation of Ignatyuk [6] and pairing and shell parameters from the Cook [7] analysis. The file of discrete level information and ground-state masses, spins and parities were taken from Firestone *et al.* [8]. The mass of the nucleus was obtained from Wapstra' data [9]. The various decay channel cross sections and emission spectra were determined by the GNASH and GSCAN codes.

3. Calculated Results and Discussion

Natural tellurium has eight stable isotopes, ^{120}Te(0.096%), ^{122}Te(2.603%), ^{123}Te(0.908%), ^{124}Te(4.816%), ^{125}Te(7.139%), ^{126}Te(18.952%), ^{128}Te(31.687%), and ^{130}Te(33.799%). We have evaluated the proton induced nuclear reaction data for Te below 60 MeV and have compared with the experimental data taken from the EXFOR. The MENDL data shown in the figures were evaluated by Shubin *et al.* [10] using the evaporation model. There are no experimental data reported up to now for the absorption cross section of

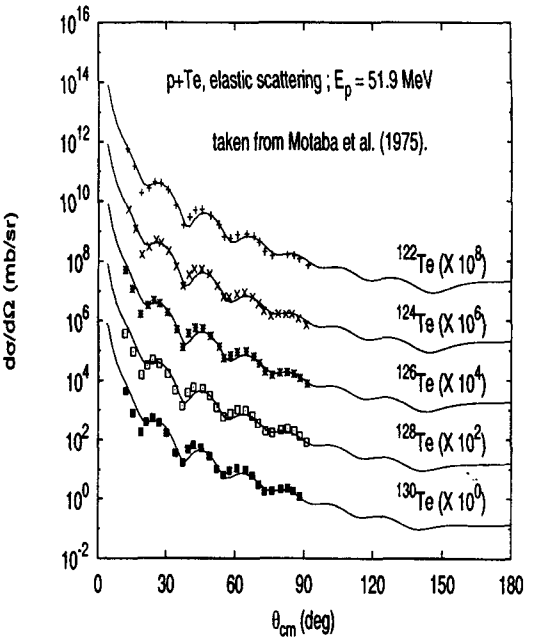

Fig. 1. Elastic Scattering Distributions for ^{122,124,126,128,130}Te. Solid Curves Show the Optical-model Predictions with Best-fit Parameters

^{122,123,124,125,126,128,130}Te.

The experimental data for the elastic scattering distributions having 26 or 27 data points were given by Matoba *et al.* [11] over several even-even nuclei, ^{122}Te, ^{124}Te, ^{126}Te, ^{128}Te and ^{130}Te, at the incident proton energy of 51.9 MeV by analyzing the scattered protons with a broad-range magnetic spectrometer. The calculated results as a function of the CMS angles of proton scattering were compared with the experimental data for ^{122,124,126,128,130}Te(p,el) reactions, as shown in figure 1. The optical parameters were obtained using the five elastic scattering data mentioned above as shown in Table 1 with χ^2 = 17.98 (^{122}Te), 18.55 (^{124}Te), 31.28 (^{126}Te), 42.40 (^{128}Te), and 39.29 (^{130}Te) over five isotopes. A total error of 10% was assumed for each experimental data.

To confirm the new optical potential parameters, the absorption cross sections and elastic scattering

Table 1. Adopted Optical Potential Parameters for Te

$V = 49.5789 - 0.12929E + 0.00282385E^2 + 0.00000\frac{N-Z}{A} + 0.00000\frac{Z}{A^{1/3}}$ (MeV),

$W_S = 27.3377 - 0.08421 + 14.247\frac{N-Z}{A}$ (MeV)

$W_V = -5.00000 + 0.24328E - 0.00467k92E^2$ (MeV),

$V_{so} = 6.04$ (MeV),

$a_r = 0.6447$ (fm), $a_S = 0.4000$ (fm), $a_V = 0.4000$ (fm), $a_{so} = 0.7400$ (fm),

$r_r = 1.1261$ (fm), $r_s = 1.1772$ (fm), $r_V = 0.9700$ (fm), $r_{so} = 1.0640$ (fm),

$r_c = 1.2500$ (fm).

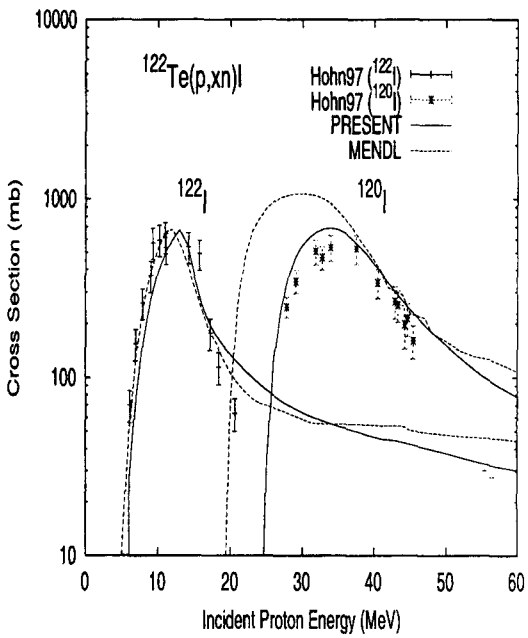

Fig. 2. Calculated and Experimentally Measured $^{122}Te(p,n)^{122}I$ and $^{122}Te(p,3n)^{120}I$ Excitation Functions

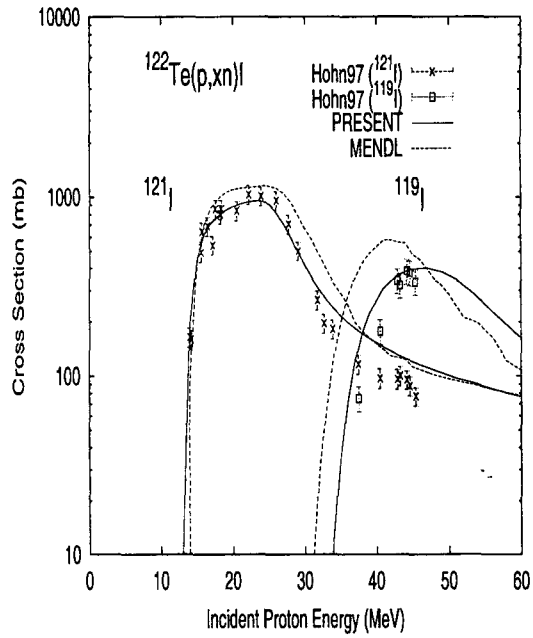

Fig. 3. Calculated and Experimentally Measured $^{122}Te(p,2n)^{121}I$ and $^{122}Te(p,4n)^{119}I$ Excitation Functions

distributions should be calculated. There are no experimental data for the absorption cross sections of tellurium. In this case, it can be obtained by summing up the cross sections of the (p,n) and (p,2n) reactions in the low energy range of the absorption cross section in which a steep incline is noticed. Below a 15 MeV proton energy, (p,n) and (p,2n) reactions are dominant, while other reactions contribute a little or not at all due to the threshold energy of these reactions. The corresponding absorption cross reactions were calculated using APMNK code with new optical potential parameters.

The measured data of the $^{122}Te(p,n)^{122}I$, $^{122}Te(p,2n)^{121}I$, $^{122}Te(p,3n)^{120}I$, and $^{122}Te(p,4n)^{119}I$ reaction cross sections were given by Hohn *et al.* [12] as shown in figures 2 and 3. The calculated results show consistent agreement with the

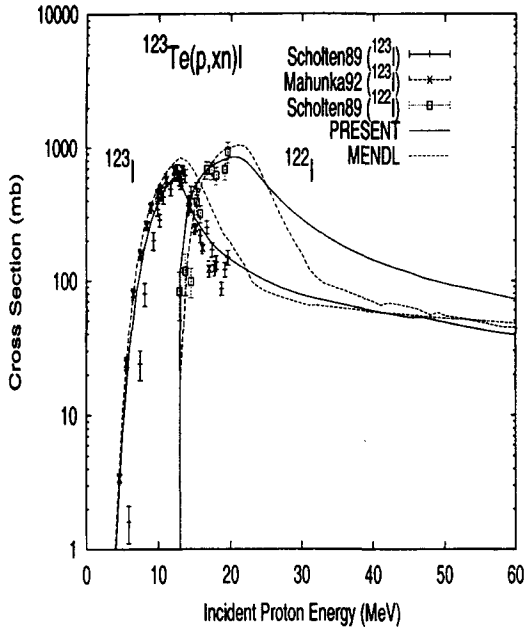

Fig. 4. Calculated and Experimentally Measured $^{123}Te(p,2n)^{122}I$ Excitation Functions

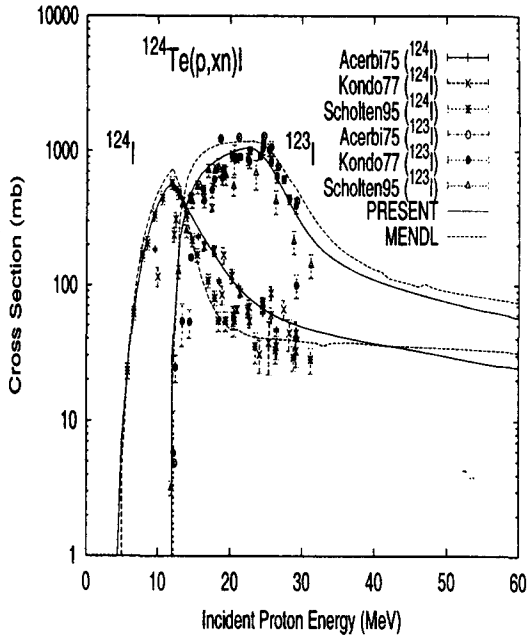

Fig. 5. Calculated and Experimentally Measured $^{123}Te(p,2n)^{123}I$ Excitation Functions

experimental data for the (p,n), (p,2n), (p,3n), and (p,4n) reactions, while the MENDL data cannot explain the cross sections for those reactions except for the (p,n) reaction. The experimental data of $^{123}Te(p,n)^{123}I$ and $^{123}Te(p,2n)^{122}I$ reactions were given by Scholten *et al.* [13]. Mahunka *et al.* [14] measured the cross section of the $^{123}Te(p,n)^{123}I$ reaction. The theoretical values of the $^{123}Te(p,n)^{123}I$, $^{123}Te(p,2n)$ ^{122}I reaction cross sections are in good agreement with the experimental data given by Scholten *et al.* In figure 4, the evaluated results for $^{123}Te(p,n)$ ^{123}I are in agreement with the experimental data for the incident proton energy of $E_p \leq 12$ MeV, while the calculated results are larger than the experimental data for $E_p \geq 12$ MeV. Nevertheless, the calculated results for $^{123}Te(p,2n)$ ^{122}I are in agreement with the experimental data as shown in figure 4. The experimental data of the $^{124}Te(p,n)^{124}I$ and $^{124}Te(p,2n)^{123}I$ reaction cross sections were given by Acerbi *et al.* [15], Kondo *et al.* [16] and Scholten *et al.* [17]. The measurements of Scholten *et al.* on the (p,n) reaction show a somewhat higher maximum cross section value and an energy shift of about 2.5 MeV as compared to the data of Kondo *et al.* A similar shift also exists between the data of Acerbi *et al.* and Kondo *et al.* Since Scholten *et al.* had characterized the energies at the compact cyclotron CV 28 and used several primary proton energies below 20 MeV, they believed their data to be more accurate. Our evaluated results reproduced the data of Scholten *et al.* well below 15 MeV, while describing those of Kondo *et al.* above 15 MeV. In figure 5, the calculated results for the overall shape and magnitude of the cross sections of the $^{124}Te(p,n)^{124}I$ and $^{124}Te(p,2n)^{123}I$ reactions are in good agreement with the

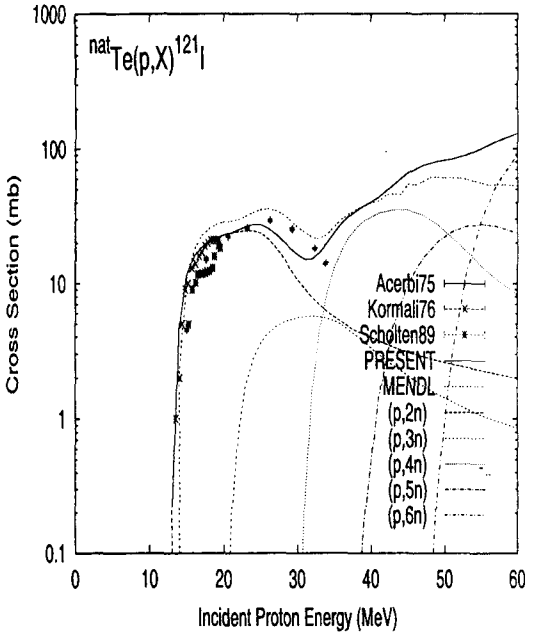

Fig. 6. Excitation Functions for the Formation of ^{121}I in the Interactions of Protons with ^{nat}Te

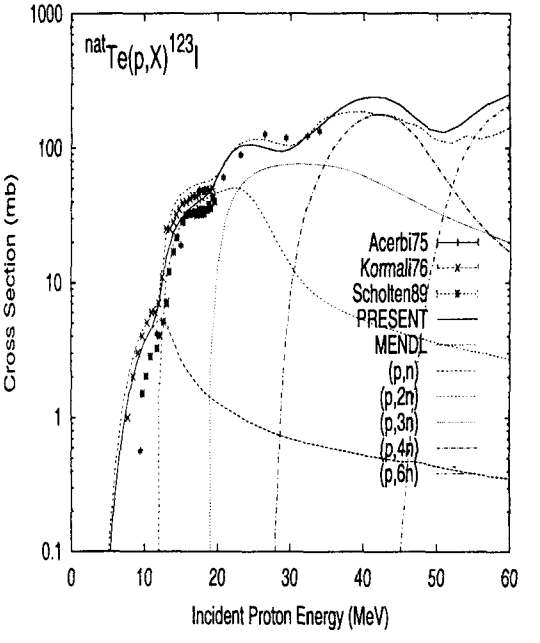

Fig. 7. Excitation Functions for the Formation of ^{123}I in the Interactions of Protons with ^{nat}Te

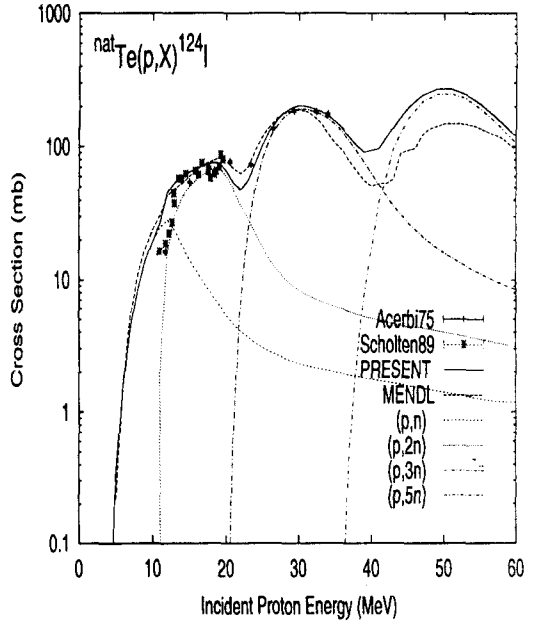

Fig. 8. Excitation Functions for the Formation of ^{124}I in the Interactions of Protons with ^{nat}Te

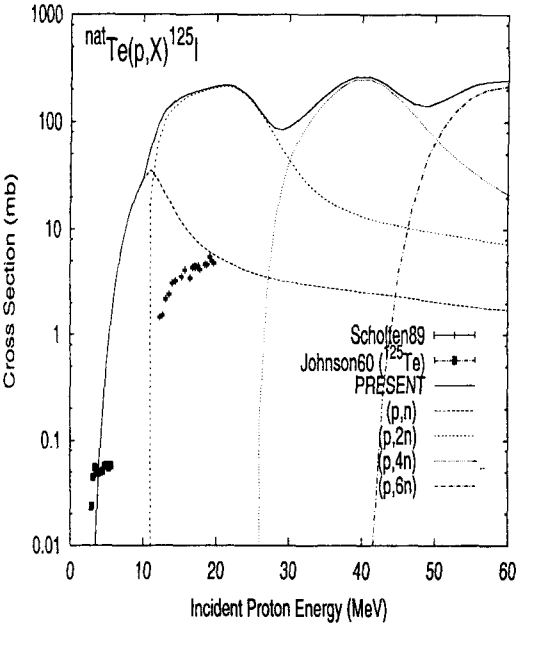

Fig. 9. Excitation Functions for the Formation of ^{125}I in the Interactions of Protons with ^{nat}Te

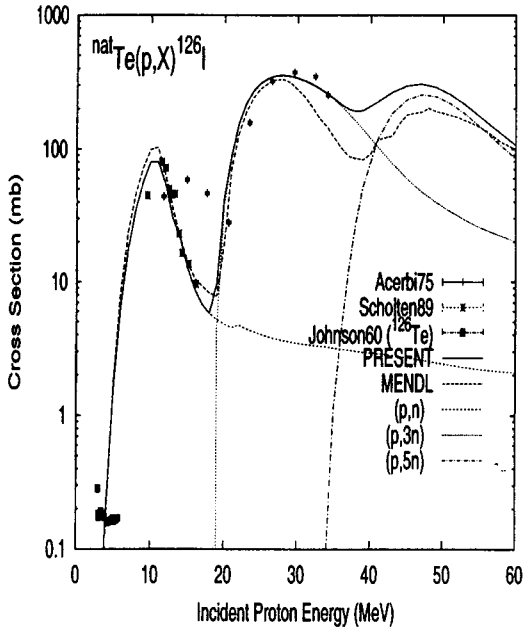

Fig. 10. Excitation Functions for the Formation of ^{126}I in the Interactions of Protons with ^{nat}Te

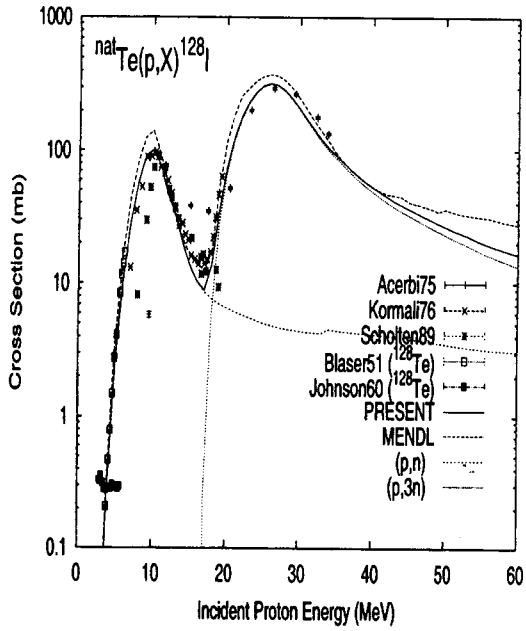

Fig. 11. Excitation Functions for the Formation of ^{128}I in the Interactions of Protons with ^{nat}Te

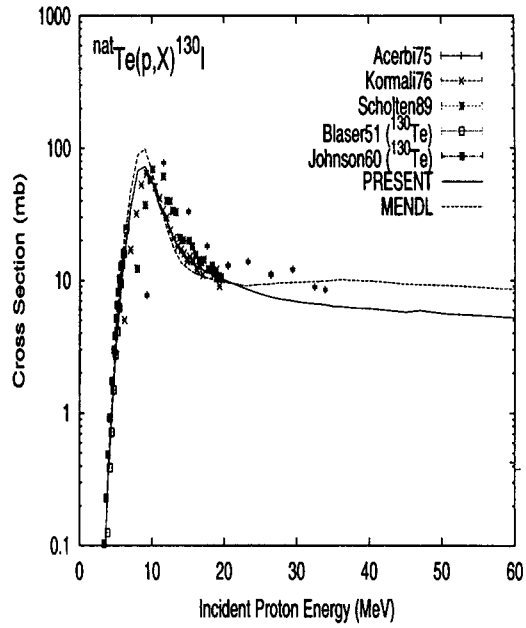

Fig. 12. Excitation Functions for the Formation of ^{130}I in the Interactions of Protons with ^{nat}Te

experimental data.

Johnson *et al.* [18] measured the cross sections of the ^{125}Te(p,n)^{125}I, ^{126}Te(p,n)^{126}I, ^{128}Te(p,n)^{128}I, and ^{130}Te(p,n)^{130}I reactions up to 6 MeV using a 4π flat-response graphite-sphere detector. Due to the existing experimental data only in the low energy region, it is difficult to demonstrate the conclusion of our calculated results. Nevertheless, as shown in figures 9,10,11 and 12, the calculated results seem to be in agreement with the experimental data of Johnson *et al.* The measured data of the ^{128}Te(p,n)^{128}I and ^{130}Te(p,n) ^{130}I reaction cross sections were also given by Blaser *et al.* [19].

There are experimental data for the (p,X) reactions on ^{nat}Te together with the evaluation results and MENDL data as shown in figures 6-12. To obtain the cross reaction sections on the ^{nat}Te-target, we need to calculate the following relation, for example,

$$\begin{aligned}\sigma[^{nat}\mathrm{Te}(p,X)^{123}\mathrm{I}] = {} & 0.009 * \sigma[^{123}\mathrm{Te}(p,n)^{123}\mathrm{I}] \\ & + 0.048 * \sigma[^{124}\mathrm{Te}(p,2n)^{123}\mathrm{I}] \\ & + 0.071 * \sigma[^{125}\mathrm{Te}(p,3n)^{123}\mathrm{I}] \\ & + 0.189 * \sigma[^{126}\mathrm{Te}(p,4n)^{123}\mathrm{I}] \\ & + 0.316 * \sigma[^{128}\mathrm{Te}(p,6n)^{123}\mathrm{I}] \\ & + 0.338 * \sigma[^{130}\mathrm{Te}(p,8n)^{123}\mathrm{I}]\end{aligned} \quad (11)$$

Scholten *et al.* [13] measured the excitation functions by the stacked-foil technique for (p,xn) reactions up to 20 MeV on natural tellurium and enriched ^{123}Te. Most of the experimental data of Scholten *et al.* are in good agreement with our evaluated results for ^{nat}Te(p,X)^{123}I, ^{nat}Te(p,X)^{124}I, ^{nat}Te(p,X)^{126}I, ^{nat}Te(p,X)^{128}I, and ^{nat}Te(p,X)^{130}I, but a few data at the threshold region are shifted by about 2 MeV, compared with the calculated results. Also, there is a considerable discrepancy between the measured data for the ^{nat}Te(p,X)^{125}I reaction and the calculated ones, as shown in figure 9. The measured data are dependent on the half-life of the residual nucleus and the energy of the emitted γ-rays by which the residual nucleus can be characterized. The γ-ray energy of 35.5 keV used to characterize the measurement for the residual nucleus, ^{125}I, is too small to extract it from a background lump of measured γ-rays, while the half-life of ^{125}I, showing longer than those of other isotopes, is not taken into account as shown in table 2. Kormali *et al.* [20] also measured the excitation functions for proton energies up to 20 MeV for ^{nat}Te(p,X)^{121}I, ^{nat}Te(p,X)^{123}I, ^{nat}Te(p,X)^{128}I, and ^{nat}Te(p,X)^{130}I. The present results reproduce the experimental data of Kormali *et al.* well over all reactions.

Table 2. Characteristics of Iodine Isotopes

Isotopes	^{120}I	^{121}I	^{122}I	^{123}I	^{124}I
Spin	2$^-$	5/2$^-$	1$^+$	5/2$^-$	2$^-$
Half-Life	1.35 h	2.12 h	3.63 m	13.7 h	4.18 d
Isotopes	^{125}I	^{126}I	^{128}I	^{130}I	
Spin	1$^+$	2$^-$	1$^+$	5$^+$	
Half-Life	59.40 d	13.11 d	24.99 m	12.36 h	

4. Summary and Conclusions

We have evaluated proton-induced nuclear data of tellurium isotopes below 60 MeV. The emphasis in this work is on a reliable estimation of the optical-model potential and the present work gives a detailed study of the excitation functions of proton induced reactions on tellurium isotopes with a global nucleon-nucleus optical model. An experimentally based global optical-model potential has broad applications in nuclear science and it has parameters that are smooth functions of the target atomic mass number and proton number, projectile type and laboratory bombarding energy. In many cases, one has used the optical-model potential for a specific projectile energy with a target. We applied a set of global optical parameters to an evaluation of the reaction cross sections of many nuclei in a broad energy range.

To obtain the new proton optical potential parameters for a proton-induced reaction, the experimental data of the absorption cross sections and elastic scattering distributions are required, but in general, the data are not good enough and are ambiguous in reliability. In this case, through other informations, such as the absorption cross section of neighboring nuclei and the emission cross sections, especially the (p, n), (p, 2n), (p, α) and (p, np) reactions, we can expect a new absorption cross section tharctically. The calculated cross-sections for using the global optical parameters should reproduce the above-mentioned absorption cross section well. The experimental data of the angle-dependent elastic scattering cross sections are used to obtain the global optical potential parameters for several tellurium isotopes.

We adjusted the level density parameters and the pair correction values of some reaction channels, as well as the composite nucleus state density constants of the pre-equilibrium model, in order to calculate the production cross sections. The calculated results for all tellurium isotopes reproduce the experimental data of the production cross sections with reasonable accuracy. This confirms that the adopted global optical potential parameters are appropriate for the calculation of the transmission coefficients needed in the statistical model based on Hauser-Feshbach formalism.

Acknowledgement

This work is supported by the Korea Ministry of Science and Technology as one of its long-term nuclear R&D programs. One of the authors (Y. HAN) is grateful to the Korea Science and Engineering Foundation for giving him an opportunity to carry out this work under the Brain Pool program.

References

1. D. Kim, Y.-O. Lee and J. Chang, "Calculation of Proton-Induced Reactions on Ti, Fe, Cu and Mo up to 60 MeV for TLA Application", *J. Korean Nuclear Soc.* **31**, 595-607 (1999).
2. Q. Shen, "APMNK - A Code for Searching Optimal Neutron and Charged Particles Optical Potential Parameters.", Private Communication (1998).
3. P.G. Young, E.D. Arthu and M.B. Chadwick, "Comprehensive Nuclear Model Calculations : Introduction to the Theory and Use of the GNASH Code", in "Workshop on Computation and Analysis of Nuclear Data Relevant to Nuclear Energy and Safety", 10 February- 13 March, Trieste, Italy (1992).
4. J. Zhang, "CUNF Code for Charged Particles Nuclear Data Calculation.", Private Communication (1995).
5. C. Kalbach, "Systematics of Continuum Angular Distributions : Extensions to Higher Energies", *Phy. Rev.* **C37**, 2350 (1988).
6. A.V. Ignatyuk, G.N. Smirenkin and A.S. Tishin, "Pheonomenological Description of the Energy Dependence of the Level Density Parameter", Sov. *J. Nucl. Phys.* **21**, 255 (1975).
7. J.L. Cook, H. Ferguson and A.R. Musgrove, "Nuclear Level Densities for Intermediate and Heavy Nuclei", *Aus. J. Phys.* **20**, 477 (1967).
8. R.B. Firestone and V.S. Shirley, "Table of Isotopes", Vol. 8, John Wiley & Sons, Inc. (1996).
9. A.H. Wapstra, " Mass Formulas and Experimental Mass Table", *At. Data Nucl. Data Tables* **39**, 281 (1988).
10. Y.N. Shubin, V.P. Lunev, A.Y. Konobeyev and A.I. Dityuk, "MENDL-2P : Proton Reaction Data Library for Nuclear Activation (Medium Energy Nuclear Data Library)", IAEA-NDS-204, IAEA Report (1998).
11. M. Matoba, M. Hyakutake, K. Yagi and Y. Aoki, "Elastic and Inelastic Scattering of 51.9 MeV Protons by Doubly Even Tellurium Nuclei", *Nucl. Phys.* **A237**, 260 (1975), **EXFOR entry E1415.**
12. A. Hohn, B. Scholten, H.H. Coenen and S.M. Qaim, "Excitation Function of (p,xn)-Reactions on Highly Enriched ^{122}Te: Relevance to the Production of ^{120g}I", **EXFOR entry D4071.**
13. B. Scholten, S.M. Qaim, G. Stocklin, "Excitation Functions of Proton Induced Nuclear Reactions on Natural Tellurium and Enriched ^{123}Te Production of ^{123}I via the ^{123}Te (p,n) ^{123}I Process at a Low-Energy Cyclotron", *Appl. Radiation and Isotopes* **40**, 127 (1989), **EXFOR entry A0473.**

14. I. Mahunka, L. Ando, P. Mikecz, A.M. Tcheltsov, I.A. Suvorov, "Excitation Functions of ^{123}Te (p,n) ^{123}I Reactions for Direct Production of ^{123}I by Small Cyclotrons", 6-th Symp. on the Medical Applications of Cyclotrons, Turku, Finland, 1-4 June 1992, **EXFOR entry D4003.**
15. E. Acerbi, C. Birattari, M. Castiglioni, F. Resmini and M. Villa, "Production of ^{123}I for Medical Purposes at the Milan AVF Cycloton", *Appl. Radiation and Isotopes* **26**, 741 (1975), **EXFOR entry A0266.**
16. K. Kondo, R.M. Lambrecht, A.P. Wolf, "Iodine-123 Production for Radiopharmaceuticals Excitation Functions of ^{124}Te (p,2n) ^{123}I and ^{124}Te (p,n) ^{124}I Reactions and the Effect of Target Enrichment on Radionuclidic Purity", *Appl. Radiation and Isotopes* **28**, 395 (1977), **EXFOR entry B0090.**
17. B. Scholten, Z. Kovacs, F. Tarkanyi, S.M. Qaim, "Excitation Functions of ^{124}Te (p,xn) ^{123,124}I Reactions from 6 to 31 MeV with Special Reference to the Production of ^{124}I at a Small Cyclotron", *Appl. Radiation and Isotopes* **46**, 255 (1995), **EXFOR entry D4019.**
18. C.H. Johnson, A. Galonsky, C.N. Inskeep, "Cross Sections for (p,n) Reactions in Intermediate-Weight Nuclei", ORNL-2910, 25 (1960) and ORNL-2501, 29 (1958), **EXFOR entry B0068.**
19. J.P. Blaser, F. Boehm, P.Marmier and P. Scherrer, *Helv. Phys. Acta* **24**, 441 (1951), **EXFOR entry P0033.**
20. S.M. Kormali, D.L. Swindle and E.A. Schweikert, "Charged Particle Activation of Medium Z Elements II. Proton Excitation Functions", *J. Rad. Chemistry* **31**, 437-450, **EXFOR entry D4073, (1976).**